Genetic and functional analyses demonstrate a role for abnormal glycinergic signaling in autism

Marion Pilorge, Coralie Fassier, Hervé Le Corronc, Anaïs Potey, Jing Bai, Stéphanie de Gois, Elsa Delaby, Brigitte Assouline, Vincent Guinchat, Françoise Devillard, et al.

Genetic and functional analyses demonstrate a role for abnormal glycinergic signaling in autism

Marion Pilorge[1,2,3], Coralie Fassier[1,2,3], Hervé Le Corronc[1,2,3,4], Anaïs Potey[1,2,3], Jing Bai[1,2,3], Stéphanie De Gois[1,2,3], Elsa Delaby[1,2,3], Brigitte Assouline[5], Vincent Guinchat[5†], Françoise Devillard[6], Richard Delorme[7], Gudrun Nygren[8], Maria Råstam[8‡], Jochen C. Meier[9], Satoru Otani[1,2,3§], Hélène Cheval[1,2,3], Victoria M. James[10,11], Maya Topf[10], T. Neil Dear[12¶], Christopher Gillberg[8], Marion Leboyer[13,14,15,16], Bruno Giros[1,2,3,17], Sophie Gautron[1,2,3#], Jamilé Hazan[1,2,3#], Robert J. Harvey[11#], Pascal Legendre[1,2,3] and Catalina Betancur[1,2,3]

[1]INSERM, U1130, Paris, France

[2]CNRS, UMR 8246, Paris, France

[3]Sorbonne Universités, UPMC Univ Paris 6, Institut de Biologie Paris Seine, Neuroscience Paris Seine, Paris, France

[4]Université d'Angers, Angers, France

[5]Centre Hospitalier Alpes-Isère, Centre Alpin de Diagnostic Précoce de l'Autisme, Saint Egrève, France

[6]Centre Hospitalier Universitaire Grenoble, Département de Génétique et Procréation, Grenoble, France

[7]AP-HP, Robert Debré University Hospital, Department of Child and Adolescent Psychiatry, Paris, France

[8]Gillberg Neuropsychiatry Centre, University of Gothenburg, Gothenburg, Sweden

[9]Technische Universität Braunschweig, Zoological Institute, Braunschweig, Germany

[10]Institute for Structural and Molecular Biology, Department of Biological Sciences, Birkbeck College, London, UK

[11]Department of Pharmacology, UCL School of Pharmacy, London, UK

[12]Leeds Institute of Molecular Medicine, University of Leeds, St. James's University Hospital, Leeds, UK

[13]INSERM U955, Institut Mondor de Recherche Biomédicale, Psychiatric Genetics, Créteil, France

[14]AP-HP, Henri Mondor-Albert Chenevier Hospital, Department of Psychiatry, Créteil, France

[15]University Paris-Est Créteil, Faculty of Medicine, Créteil, France

[16]Fondation Fondamental, Créteil, France

[17]Douglas Mental Health University Institute, Department of Psychiatry, McGill University, Montreal, Quebec, Canada

[#]These authors contributed equally to this work

[†]Current address: Department of Child and Adolescent Psychiatry, Pitié-Salpêtrière Hospital, Paris, France

[‡]Current address: Department of Clinical Sciences, Child and Adolescent Psychiatry, Lund University, Lund, Sweden

[§]Current address: Center of Medical Education, Faculty of Health Sciences, Ryotokuji University, Urayasu, Japan

[¶]Current address: South Australian Health and Medical Research Institute, Adelaide, Australia

Correspondence:

Catalina Betancur, Neuroscience Paris Seine, Université Pierre et Marie Curie, case courrier 37, 7 quai Saint Bernard, 75005 Paris, France. E-mail: catalina.betancur@inserm.fr

Running title: Rare *GLRA2* mutations in autism

Abstract

Autism spectrum disorder (ASD) is a common neurodevelopmental condition characterized by marked genetic heterogeneity. Recent studies of rare structural and sequence variants have identified hundreds of loci involved in ASD, but our knowledge of the overall genetic architecture and the underlying pathophysiological mechanisms remains incomplete. Glycine receptors (GlyRs) are ligand-gated chloride channels that mediate inhibitory neurotransmission in the adult nervous system but exert an excitatory action in immature neurons. GlyRs containing the α2 subunit are highly expressed in the embryonic brain, where they promote cortical interneuron migration and the generation of excitatory projection neurons. We previously identified a rare microdeletion of the X-linked gene *GLRA2,* encoding the GlyR α2 subunit, in a boy with autism. The microdeletion removes the terminal exons of the gene (*GLRA2*Δex8-9). Here, we sequenced 400 males with ASD and identified one *de novo* missense mutation, p.R153Q, absent from controls. *In vitro* functional analysis demonstrated that the GLRA2Δex8-9 protein failed to localize to the cell membrane, while the R153Q mutation impaired surface expression and dramatically reduced sensitivity to glycine. Very recently, an additional *de novo* missense mutation (p.N136S) was reported in a boy with ASD, and we show that this mutation also reduced cell surface expression and glycine sensitivity. Targeted *glra2* knockdown in zebrafish induced severe axon branching defects, rescued by injection of wild-type but not GLRA2Δex8-9 or R153Q transcripts, providing further evidence for their loss-of-function effect. *Glra2* knockout mice exhibited deficits in object recognition memory and impaired long-term potentiation in the prefrontal cortex. Taken together, these results implicate *GLRA2* in non-syndromic ASD, unveil a novel role for *GLRA2* in synaptic plasticity and learning and memory, and link altered glycinergic signaling to social and cognitive impairments.

INTRODUCTION

Autism spectrum disorder (ASD) is a clinically and genetically heterogeneous neurodevelopmental condition defined by impairments in social communication and interaction, accompanied by repetitive behaviors and restricted interests. Rare and very rare copy number variants (CNVs) and sequence variants, both inherited and *de novo*, affecting hundreds of loci have been implicated in ASD.[1-5] Many of these variants involve genes on the X chromosome,[2] which may partially explain the excess of affected males over females observed in ASD (4:1). To date, nearly 100 X-linked genes have been associated with intellectual disability and other neurodevelopmental disorders including autism, primarily in hemizygous males.[6] A large number of genes implicated in syndromic and non-syndromic ASD are involved in synaptic function, highlighting this as a convergent pathway dysregulated in ASD.[7] However, despite recent advances, the underlying genetic determinants are unknown in the majority of cases and our understanding of the pathophysiological mechanisms leading to ASD remains incomplete.

Glycine receptors (GlyR) are members of the Cys-loop ion channel superfamily that also includes γ-aminobutyric acid type A ($GABA_A$), nicotinic acetylcholine and serotonin 5-HT_3 receptors. GlyR typically consists of pentameric combinations of alpha (α1-α4) and beta (β) subunits forming a central pore that selectively controls transmembrane

flux of chloride.[8] Functional GlyRs can be formed as homomers comprising five α subunits, or as heteromers comprising α and β subunits. Each subunit contains a large N-terminal extracellular domain, which harbors the ligand binding site, and four transmembrane domains, termed TM1-TM4. In humans, *GLRA1*, *GLRA2*, and *GLRA3* encode α subunits (*GLRA4* is a pseudogene), whilst *GLRB* encodes the β subunit. GlyR α subunits exhibit distinct spatial and temporal expression patterns in the central nervous system (CNS). The α2 subunit is widely expressed in embryonic and perinatal CNS and expression markedly decreases after birth,[9,10] suggesting a role for α2-containing GlyR in neuronal development. By contrast, α1 and α3 GlyRs mediate the majority of glycinergic neurotransmission in the adult spinal cord and brain stem, where they are involved in hyperekplexia (startle disease)[11] and inflammatory pain,[12] respectively. GlyR α3 is also expressed in the hippocampus, where it has been implicated in temporal lobe epilepsy.[13] Although known as the main inhibitory neurotransmitters in the adult CNS, glycine and GABA have a depolarizing and excitatory action in immature neurons due to the inverted chloride gradient during development.[14,15] At these early stages, embryonic GlyRs and $GABA_A$ receptors are located extrasynaptically and can be tonically activated by paracrine release of endogenous agonists.[14,16,17] The subsequent increase in intracellular Ca^{2+} generates spontaneous electrical activity that can shape neuronal network formation.[18] The developmental role of GABA in neuronal proliferation, migration, and differentiation has been widely documented,[19-21] and a growing body of evidence supports similar neurotrophic effects for glycine in the developing CNS[22-26] and retina.[27] In particular, recent studies have demonstrated the role of GlyR α2 in proliferation and neuronal migration during cortical development.[25,26]

As part of a large CNV screen in ASD,[28] we previously identified a rare microdeletion of *GLRA2* in a boy with autism, absent from controls. Here, we screened a cohort of 400 males with ASD for *GLRA2* sequence variants and identified a *de novo* missense mutation, R153Q. We next examined the cell-surface localization and electrophysiological properties of the deleted (*GLRA2*Δex8-9) and mutated (R153Q) GLRA2 proteins in transfected CHO cells to assess the functional impact of the mutations. We also characterized an additional, recently described *de novo* missense *GLRA2* mutation[5] in CHO cells. Using molecular modeling, we further investigated the effect of the R153Q mutation on receptor function. To determine the functional consequences of the ASD-related *GLRA2* mutations *in vivo*, we knocked down *glra2* expression in zebrafish embryos and performed rescue experiments with human wild-type and mutated *GLRA2* transcripts. Finally, we investigated the effects of *Glra2* disruption on behavior and synaptic plasticity in mice. Overall, our results implicate the *GLRA2* gene in ASD and link alterations in glycine-mediated signaling to the social and cognitive dysfunction associated with ASD.

MATERIALS AND METHODS

Subjects

Patients were recruited by the Paris Autism Research International Study (PARIS) at specialized clinical centers in France and Sweden.[29] All patients were evaluated by psychiatrists and diagnosed based on clinical evaluation and DSM-IV criteria. Subjects were assessed with the Autism Diagnostic Interview-Revised (ADI-R) and the Asperger Syndrome Diagnostic Interview;[30] those recruited more recently were also assessed with the Autism Diagnostic Observation Schedule (ADOS). At the time of inclusion, patients were screened for genetic disorders associated with

autism; investigations included karyotype, molecular genetic testing for fragile X syndrome, and metabolic screening; brain imaging and EEG were performed when possible. In addition, subjects were screened for microdeletion/microduplication syndromes using multiplex ligation-dependent probe amplification (MLPA) and/or chromosomal microarray analysis. Patients with known genetic disorders were excluded from subsequent analysis. All families provided informed consent and the research was approved by the ethics committees of the participating institutions (Comité de Protection des Personnes Ile-de-France VI, Paris, France, and Ethical Review Board in Gothenburg, Sweden).

The sample of 400 independent males screened for *GLRA2* mutations included 334 probands from simplex families and 66 from multiplex families (with two or more affected siblings); 336 met criteria for autism, 44 for Asperger syndrome, and 20 for pervasive developmental disorder not otherwise specified; 42% had very limited or no language; 62% had intellectual disability (IQ<70), and 8.5% had a history of epilepsy. The mean age at inclusion was 11.8 years (3-39 years). Most patients were Caucasian (90%).

Mutation screening

All *GLRA2* coding exons and intron-exon boundaries were PCR-amplified and sequenced using DNA extracted from blood or B lymphoblastoid cell lines. See Supplementary Methods for details. Where mutations were shown to have arisen *de novo*, we verified maternity and paternity by genotyping both parents and the subject at several microsatellite loci.

Reference sequences

GenBank accession numbers for genomic and protein sequences for *GLRA2* are NM_002063.3 and NP_002054.1, respectively. Note that amino acid sequence numbering is given with the signal peptide; residues are numbered starting at the initiator methionine, in accordance with the nomenclature recommendations of the Human Genome Variation Society (HGVS, http://www.hgvs.org). The first amino acid after signal peptide cleavage is residue number 28. Genomic locations are based on GRCh37/hg19.

Accession numbers for genomic and protein sequences for *Glra2* in mice are NM_183427.4 and NP_906272.1, and for *glra2* in zebrafish NM_001167899.1 and NP_001161371.1.

GLRA2 constructs

GLRA2 cDNA was generated from human hippocampus poly A^+ RNA (Clontech, Mountain View, CA, USA) and cloned into pEGFP-N1 vector (Clontech) using *Not*I, which excises the enhanced green fluorescent protein (EGFP) coding sequence. Mutations were performed using the QuikChange II site-directed mutagenesis kit (Stratagene, La Jolla, CA, USA) according to the manufacturer's instructions, and positive clones were identified by DNA sequencing. The GLRA2 truncated mutant was produced to end at amino acid 310, immediately followed by 6 amino acids (VRNLA*), resulting in a 316 amino acid truncated protein, like in in Patient 1 (Figure 2a). For the GLRA2 construct mimicking the mutation in Patient 2, the arginine residue at position 153 was changed to glutamine (R153Q) (Figure 2a). For the additional *de novo* missense mutation reportedly recently in an ASD patient,[5] the asparagine at position 136 was changed to serine (N136S). Chinese hamster ovary (CHO) cells were co-transfected with the different GLRA2 constructs and EGFP cDNA using FuGENE 6 Transfection Reagent (Roche, Indianapolis, IN, USA). CHO cells were recorded or immunolabeled 48 h after transfection. Cells were routinely tested for mycoplasma contamination.

Whole-cell recordings

Whole-cell patch-clamp recordings of transfected CHO cells were performed at room temperature using an Axopatch 200B amplifier (Molecular Devices, Sunnyvale, CA, USA) in saline solution containing (in mM): 126 NaCl, 1.2 NaH_2PO_4, 4.5 KCl, 10 glucose, 2 $CaCl_2$, 1 $MgCl_2$, and 10 HEPES (pH 7.2). Patch-clamp electrodes (4-6 MΩ) contained an internal solution with the following composition (in mM): 130 CsCl, 4 $MgCl_2$, 4 Na_2ATP, 10 EGTA, and 10 HEPES (pH 7.2).

Transfected cells were selected according to their EGFP expression under UV light. Data were low-pass filtered at 2 KHz, digitized at 20 kHz with a Digidata 1322A interface, and acquired using PClamp 10 software (Molecular Devices). Glycine was applied using 0.5 mm diameter quartz tubing positioned 1 mm away from the recording area.[17] The quartz tubing was connected using a manifold to reservoirs filled with saline solution or with different concentrations of glycine (solution exchange times ≤ 30 ms). Different glycine concentrations were applied to CHO cells expressing wild-type or mutant GlyR α2 subunits to control possible amplitude rundown. All compounds were purchased from Sigma-Aldrich (Saint-Quentin Fallavier, France). Analyses were performed off-line with PClamp 10 software or Axograph X.1.3.5 software (AxoGraph Scientific, Sydney, Australia).

Immunohistochemistry

Transfected CHO cells were immunolabeled using goat polyclonal antibodies against the N-terminal 18 amino acids of the human GlyR α2 subunit (GlyR α2 N-18: SC-17279; Santa Cruz Biotechnology, Santa Cruz, CA, USA). For details see Supplementary Methods.

Cell surface biotinylation

Surface proteins of transfected CHO cells were biotinylated using the Pierce Cell Surface Protein Isolation Kit (Thermo Scientific, Rockford, IL, USA) and analyzed using western blotting. For details see Supplementary Methods.

Molecular modeling of the GlyR α2 homomer

Fold recognition of human GlyR α2 subunit was performed with HHPred.[31] The structure of the *Caenorhabditis elegans* glutamate-gated chloride channel α (GluCl) (PDB: 3RIF) was identified as the best template. A profile-profile alignment between the human GlyR α2 subunit and the *C. elegans* GluCl α subunit (chain A) was generated using MUSCLE web server (www.ebi.ac.uk/Tools/msa/muscle), resulting in 42% sequence identity. Based on this alignment, 50 homology models of human GlyR α2 subunit were built using MODELLER-9v10 (http://salilab.org/modeller/) and assessed with the DOPE statistical potential score. The model based on the lowest score (Z score = –0.174) was selected. Additional evaluation using the ProSA web server (https://prosa.services.came.sbg.ac.at/prosa.php) showed that the model quality (Z score = –4.95) fell within a range typically found for native proteins of similar size, demonstrating the high quality and reliability of the model. Using the Chimera molecular visualization and analysis software (http://www.cgl.ucsf.edu/chimera/), a glycine molecule was docked into an approximate position within the predicted binding site, using structural information about the binding of glutamate in the GluCl obtained from the crystal structure (PDB: 3RIF), and experimental evidence of residues in GlyR α1 that are known to interact with the glycine ligand.[32] The substitution R153Q was modeled into the GlyR α2 homology model using the *swapaa* command, taking into account the highest rotamer probability (based on the Dunbrack backbone-dependent rotamer library), the highest number of H-bonds, and the lowest clash score.

Zebrafish analyses

For knock-down analysis of zebrafish *glra2*, two-cell stage wild-type zebrafish embryos were injected with antisense morpholino oligonucleotides directed against the *glra2* translation initiation site (*glra2* MO) at 1 pmol per embryo and analyzed at 28 h post-fertilization by standard immunostaining procedures. For rescue experiments, the wild-type, mutated, and deleted versions of human *GLRA2* transcripts were co-injected at 100 pg in one-cell stage zebrafish embryos together with the *glra2* MO. Additional details are given in the Supplementary Methods.

Mice

Glra2 mutant mice were generated by T.N.D. and R.J.H. and maintained in our laboratory in Paris on a C57BL/6J background (see Supplementary Methods). Only males were used for the behavioral, molecular, and

electrophysiological studies. All mice were between 9 and 20 weeks of age at the start of the behavioral experiments. All experiments were conducted in accordance with the European Communities Council Directive (86/609/EEC) and approved by the local animal ethics committee (Comité d'éthique en expérimentation animale Charles Darwin, C2EA–05).

Behavioral assays

Glra2 hemizygous (*Glra2*$^{-/Y}$) males and wild-type (*Glra2*$^{+/Y}$) littermates were housed in groups of three to four per cage (33 x 15 x 13 cm) with free access to food and water in a temperature- and humidity-controlled animal facility maintained on a 12 h light/dark cycle. Sample size was chosen based on previous experience with behavioral assays. All tests were performed blind to genotype. Cages and subjects within a cage were tested in random order. A detailed description of experimental procedures is provided in the Supplementary Methods.

***Ex-vivo* electrophysiology**

Male *Glra2*$^{-/Y}$ mice and wild-type littermates were decapitated and the brain was rapidly removed from the skull. Coronal slices (400 µm) containing the prelimbic area (1.94-2.8 mm from the bregma) were sectioned with a vibratome (Campden Instruments, Loughborough, UK) in chilled oxygenated (95% O_2/5% CO_2) artificial cerebrospinal fluid (ACSF) containing in mM: 124 NaCl, 2 KCl, 26 $NaHCO_3$, 1.15 KH_2PO_4, 1 $MgCl_2$, 2 $CaCl_2$, and 11 D-glucose. Slices were allowed to recover in oxygenated ACSF at room temperature for at least 3 h before recording. Experiments were performed in a submersion recording chamber with continuous perfusion (1 ml/min) of warmed ACSF (32° C).

Experiments were conducted in the following order: recording of stable baseline field excitatory postsynaptic potentials (fEPSPs) for at least 20 min, delivery of high-frequency stimulation (50 pulses at 100 Hz, 5 times with 3 min interval) to induce plasticity, followed by response monitoring for 50 min post-conditioning. The stimulating and recording electrodes were both placed on the surface of layer I-II, as described.[33] Single stimulations (monophasic constant current square pulses; 100 µs width) were applied through a bipolar stimulating electrode (teflon-coated tungsten, A-M Systems, Sequim, WA, USA). Recordings were made with glass micropipettes filled with 3 M NaCl. fEPSPs were evoked at 0.033 Hz, and the response size was set at 60% of the maximum amplitude, which was about 0.7-0.8 mV with 30-40 µA stimulus intensities. All evoked responses were fed to an amplifier in current-clamp mode and digitized at 10 kHz through a Digidata 1322A interface (Molecular Devices) using Elphy data-acquisition software (CNRS, Gif sur Yvette, France). The initial slope of the EPSP (1 ms period from its onset, mV/ms) was calculated for each individual EPSP as previously described.[33] Statistical comparisons between the averaged slopes of the last 10 min after high-frequency stimulation and the baseline responses were performed for each genotype using Wilcoxon's matched-pairs signed ranks test.

Statistics

Values are shown as mean ± SEM. Data were analyzed using unpaired two-tailed Student's *t*-test (with equal or unequal variance, as appropriate) or analysis of variance (ANOVA). The Mann-Whitney U test was used where data were not normally distributed. Time course data without normal distribution were analyzed by two-way repeated-measures ANOVA after data transformation. Analysis of *ex vivo* electrophysiological data was performed using Wilcoxon's signed ranks test. Statistical analyses were done using Prism 5 (GraphPad Software, San Diego, CA, USA). Full statistical tests are presented in Supplementary Table S6.

RESULTS

GLRA2 mutations in ASD patients

In a genome-wide CNV study of 996 ASD individuals using Illumina 1M SNP microarrays,[28] we identified a microdeletion of *GLRA2* (chrX:14693216-14836199, hg19) in a boy with non-syndromic autism (Patient 1). This boy

had language delay with functional language, and low average IQ (verbal IQ 93, performance IQ 75, and full-scale IQ 82); the physical exam was normal, with no dysmorphic features (see Supplementary Clinical Description for further details). The deletion was inherited from his healthy mother, consistent with X-linked recessive transmission. The 151-kb deletion (*GLRA2*$^{\Delta ex8\text{-}9}$) encompasses the last two exons of *GLRA2* (Figure 1a), and is predicted to result in loss of transmembrane domains TM3 and TM4. The deletion was validated using qPCR and the breakpoint was localized to intron 7 after sequencing the junction fragment (Figure 1b, c, and Supplementary Figure S1). The endpoints of the deletion arose in regions lacking extensive homology, suggesting that this is a non-recurrent event. Reverse transcription of mRNA from blood samples of Patient 1 and his mother, followed by *GLRA2* cDNA amplification, demonstrated the presence of a truncated transcript, indicating the mutated allele escapes nonsense-mediated mRNA decay (Supplementary Figure S2a, b, c). The deletion of the last two exons results in the incorporation of intron 7, leading to a stop codon, as shown by RNA sequencing (Supplementary Figure S2d). The translation product would terminate with five additional amino acids followed by a stop codon (VRNLA*) (Supplementary Figure S2d). The patient's mother had a normal, non-skewed X chromosome inactivation pattern (not shown). No other *GLRA2* deletions were observed in 2245 ASD cases, 4875 parents, and 4768 controls analyzed by the Autism Genome Project.[3,28] Furthermore, *GLRA2* deletions were absent from 1124 ASD probands[1] and 11004 controls from previous studies (Supplementary Table S1), indicating that *GLRA2* deletions are very rare events.

To further delineate the role of *GLRA2* mutations in ASD, we used direct sequencing to investigate the coding regions and splice site junctions of this gene in 400 affected males. We identified a *de novo* missense mutation, c.458G>A, leading to the amino acid substitution p.R153Q in one subject (Figure 1d). Patient 2 had non-syndromic autism, severe language delay with functional language, mild intellectual disability (verbal IQ 63, performance IQ 67, and full-scale IQ 63), and generalized tonic-clonic seizures starting at 18 years (Supplementary Clinical Description). No clinically-relevant CNVs were identified in this patient. The patient has an older sister with autism who does not carry the *GLRA2* mutation (Supplementary Clinical Description), which suggests intrafamilial heterogeneity, a common finding among multiplex families with autism[34] and not unexpected given the profound etiological heterogeneity underlying ASD and the high rate of the disorder. The mutation affects a highly conserved amino-acid residue, unchanged in protein sequences of GLRA2 in vertebrates, as well as in GLRA1 and GLRA3 in humans (Figure 1e). This change was predicted to be damaging by PolyPhen-2, SNPs&GO, MutPred, PANTHER, and SIFT (Supplementary Table S3). The R153Q substitution was absent from 404 unaffected fathers of ASD probands from our cohort, and was not listed in dbSNP (build 138), the 1000 Genomes database, or the Exome Variant Server (Supplementary Table S2). In total, the p.R153Q mutation was absent from 18349 control X chromosomes. Furthermore, the mutation has not been reported in 4032 cases with ASD, or in 3302 patients with schizophrenia, intellectual disability or epilepsy from previous studies (Supplementary Table S2). No other likely pathogenic mutations in *GLRA2* were identified in our 400 ASD males (Supplementary Table S4), in >4000 males with ASD or other neurodevelopmental disorders, or in 5029 male controls (Supplementary Table S2). Since the completion of our studies, an additional *de novo* missense mutation in *GLRA2* (p.N136S) was reported in a male with ASD in a whole-exome sequencing study of over 2500 simplex families.[5] This mutation affects a highly conserved residue

located in the ligand-binding domain, and is predicted to be deleterious by multiple algorithms (Supplementary Table S3). A missense variant (p.R350L) predicted to be damaging was reported in a female with ASD[35] (Supplementary Tables S2, S3), and was inherited from her healthy mother, consistent with our observation that *GLRA2* mutations are not associated with a phenotype in females. Likewise, three missense variants reported in healthy males in the Exome Variant Server are predicted to be benign by the majority of *in silico* prediction tools, whereas potentially damaging missense variants are only reported in heterozygous females (Supplementary Table S3).

GLRA2* mutations have loss-of-function effects *in vitro

We used *in vitro* studies to analyze the functional impact of the *GLRA2* exon 8-9 deletion and R153Q substitution found in ASD patients. We generated truncated ($GLRA2^{\Delta ex8-9}$) and mutated ($GLRA2^{R153Q}$) constructs as shown in Figure 2a, and co-transfected them with EGFP cDNA in CHO cells. As TM3 and TM4 are crucial for anchoring of the protein to the membrane, we predicted that the $GLRA2^{\Delta ex8-9}$ truncated mutant would exhibit loss of membrane localization. Consistent with this, the wild-type and $GLRA2^{R153Q}$ proteins were both observed at the plasma membrane of transfected cells, whereas $GLRA2^{\Delta ex8-9}$ was undetectable at the cell surface (Figure 2a) and was mislocalized to the cytoplasm in permeabilized cells (Supplementary Figure S3). To determine whether the $GLRA2^{R153Q}$ mutation affected the number of GlyR α2 on the cell surface, we isolated biotinylated surface receptors and analyzed them by western blotting. $GLRA2^{R153Q}$ induced a 56% decrease in surface expression compared to wild-type GLRA2 (Supplementary Figure S4). Quantification of the intracellular fraction also revealed reduced expression of the R153Q mutant (–32%), suggesting decreased synthesis or increased degradation. Previous studies of recessive *GLRA1* missense mutations in hyperekplexia showed reduced stability of receptor proteins resulting in reduced cell surface accumulation.[36]

The p.R153Q mutated residue is located in the N-terminal extracellular domain of the protein, consistent with a potential role in glycine binding and GlyR activation. To determine the functional properties of the two mutant GlyRs, we analyzed whole-cell currents evoked by the application of glycine on transfected cells. As shown in Figure 2, the minimum concentration of glycine able to evoke a whole-cell current was ~100 times higher in cells expressing the $GLRA2^{R153Q}$ mutant than in cells expressing the wild-type GlyR α2 subunit. Expression of $GLRA2^{R153Q}$ was associated with a rightward shift in the dose-response curve, with a significantly higher EC_{50} value (mutant EC_{50}=8.9 ± 0.9 mM, *n*=7; wild-type EC_{50}=0.056 ± 0.002 mM, *n*=13; Mann-Whitney U test, $P<0.01$; Figure 2b, c; Supplementary Table S5), indicating a dramatically reduced sensitivity to glycine. This result implies that GlyRs containing the R153Q mutation are unlikely to be significantly activated in response to glycine release under physiological conditions in the developing CNS (≤100 µM extracellular glycine). As expected, application of glycine at high concentration (30 mM) on cells expressing $GLRA2^{\Delta ex8-9}$ did not evoke any current (*n*=5), due to the lack of cell surface expression of the deleted protein. To further study the effects of the R153Q substitution in Patient 2, we generated a homology model of the human GlyR α2 homomer. The model predicts that R153Q abolishes critical hydrogen bonds in the glycine-binding site, leading to the destabilization of the ligand-binding region and loss of function (Figure 2d, e). Taken

together, our results demonstrate that both the *GLRA2* deletion and the R153Q mutation identified in patients with ASD dramatically impair GlyR α2 function *in vitro*.

ASD-associated mutations in *GLRA2* fail to rescue axon defects caused by *glra2* knockdown in zebrafish

To assess whether the deletion and the R153Q mutation affect GLRA2 function *in vivo*, we knocked down the zebrafish orthologue *glra2* and subsequently performed rescue experiments with human wild-type or mutated *GLRA2* transcripts. We first characterized a prominent and reproducible phenotype in 24-hours-post-fertilization (hpf) embryos injected with an antisense morpholino oligonucleotide targeted against *glra2* translation start site. The knockdown of *glra2* led to obvious hyperbranching of spinal motor axons compared to controls (three independent experiments, n >30 embryos per group; Figure 3a). To ascertain the specificity of this defect of spinal motor neurons (SMN), we combined *in situ* hybridization experiments and RT-PCR analysis on fluorescence-activated cell -sorted SMN to confirm the presence of *glra2* in this neuronal population (Supplementary Figure S4), and performed rescue experiments by co-injecting human wild-type *GLRA2* mRNA with *glra2* morpholino. Human wild-type *GLRA2* transcript fully rescued the multiple aberrant branching of zebrafish *glra*-depleted SMN, confirming the specificity of the morphant phenotype. In contrast, injection of the deleted or mutated *GLRA2* transcripts failed to rescue SMN axon outgrowth defects in morphant embryos (four independent experiments, n >40 embryos per group; Figure 3b, c), establishing that both the deletion and the mutation disrupt the normal function of GLRA2 *in vivo*.

***Glra2* knockout mice have impaired learning and memory and abnormal cortical synaptic plasticity**

Autism is associated with core social deficits as well as repetitive behaviors and/or restricted interests, however, additional cognitive and behavioral deficits are common, including intellectual disability, gross and fine motor deficits, and heightened anxiety. To further investigate the *in vivo* function of GlyR α2, we characterized male *Glra2* knockout mice in a complete battery of behavioral tests assessing various aspects of brain function and ASD-related behaviors, including diverse social and motor abilities, anxiety, repetitive and stereotypic behaviors, learning, and memory. Mutant mice had normal adult body and brain weight, were fertile, and had a normal life span. Locomotor activity in a novel cage and in the open-field was similar in *Glra2*$^{-/Y}$ and wild-type mice (Supplementary Figure S6a, b). Motor coordination on the accelerating rotarod and motor strength in the wire hang test were both normal (Supplementary Figure S6c, d). Anxiety-like behaviors, tested in the light-dark box and the elevated plus maze, were indistinguishable in hemizygous *Glra2*$^{-/Y}$ mice and wild-type littermates (Supplementary Figure S6e, f). No differences between genotypes were observed in social behavior assessed in four tests: sociability (social versus inanimate preference test) and preference for social novelty (familiar versus stranger mouse), olfactory habituation/dishabituation to non-social and social odors, social interaction with juveniles, and nest formation (Supplementary Figure S7a-d). Similarly, no increase in repetitive behavior in the hole board and the marble burying tests was observed in *Glra2*$^{-/Y}$ mice compared to wild-type animals (Supplementary Figure S6g, h). Furthermore, no

enhanced stereotypies or abnormal grooming were observed in *Glra2* mutant mice (not shown). For the complete statistical analyses of all behavioral tests, see Supplementary Table S6.

We next tested learning and memory abilities of *Glra2*$^{-/Y}$ mice. When assessed in the novel object recognition task, 10 min after the familiarization phase, wild-type mice spent significantly more time exploring the novel object, whereas *Glra2*$^{-/Y}$ mice showed no preference (Figure 4a), indicating impaired short-term memory. This deficit was confirmed in three additional cohorts of mice and was also observed in the long-term memory version of the task, after a delay of 24 h (Figure 4a), indicating that *Glra2*$^{-/Y}$ mice have short-term and long-term memory impairments. In contrast, *Glra2*$^{-/Y}$ mice did not display deficits in spatial learning in the novel location recognition test, either 10 min or 24 h after the familiarization phase (Figure 4b). To further assess the spatial learning and memory of *Glra2*$^{-/Y}$ mice, we evaluated their performance in the Morris water maze. Mean escape latencies to find the platform during training in the hidden-platform task indicated similar spatial learning in wild-type and mutant mice (Supplementary Figure S8a). Moreover, both genotypes spent significantly more time in the target quadrant during memory probe trials conducted either 10 min (Figure 4c) or 24 h after training (Supplementary Figure S8b, c). During reversal training, both genotypes learned the new platform location within two days and showed similar selective quadrant search in the probe trials (Figure 4c, Supplementary Figure S8b, c). In conclusion, *Glra2*$^{-/Y}$ mice showed impaired learning and memory in the novel object recognition task, whereas spatial learning and memory in the novel location recognition task and in the Morris water maze were normal.

To test whether the disruption of *Glra2* altered synaptic plasticity, we measured long-term potentiation in prefrontal cortex slices prepared from *Glra2*$^{-/Y}$ and wild-type mice. After high-frequency stimulation, we observed that long-term potentiation was significantly impaired in *Glra2* mutant mice compared to controls (Figure 4d). These findings suggest that defective glycinergic signaling results in abnormal plasticity in the prefrontal cortex, a region consistently implicated in ASD.[37-39]

DISCUSSION

Given the extreme locus heterogeneity in ASD, it can be very challenging to identify sufficient repeated instances of mutations in the same gene to determine pathogenicity. Additional lines of evidence are therefore required to identify disease-causing variants and understand their functional impact. Combining genetic analysis and extensive functional studies represents a powerful strategy to identify genes, while providing insights into the molecular mechanisms underlying ASD.

In vitro functional characterization of the *GLRA2* deletion and missense mutation identified in two patients with ASD revealed two mutational mechanisms. The *GLRA2* deletion prevented cell surface expression of GlyR α2 due to the loss of TM3 and TM4 domains. The R153Q mutation did not appear to impair plasma membrane expression in confocal immunofluorescence analysis, but quantification using biotinylation assays revealed markedly reduced cell-surface expression of the receptor. In addition, R153Q dramatically reduced glycine sensitivity, presumably through the disruption of hydrogen bonds with T238 that are required to stabilize the ligand-binding region. Of note,

substitution of the equivalent amino acid in *GLRA1*, p.R147 (referred in the literature as p.R119 when numbered without the signal peptide), in site-directed mutagenesis studies, also led to a dramatic reduction in apparent glycine affinity.[40,41] Our data are consistent with previous studies showing that most hyperekplexia-causing mutations in *GLRA1* and *GLRB* result either in disrupted surface expression or altered glycine efficacy.[42] Overall, our results demonstrate that *GLRA2* mutations identified in patients with ASD lead to a loss-of-function of GlyR α2, either by affecting its subcellular localization or by reducing agonist sensitivity.

Our loss-of-function and rescue analyses during development of the zebrafish further confirmed the significant impact of the deletion and R153Q missense mutation on the function of GlyR α2 *in vivo*.[43] The knockdown of *GLRA2* zebrafish orthologue resulted in a prominent defect of spinal motor axon outgrowth and branching, in agreement with a previous *in vitro* study showing that the blockade of GlyR increased neurite outgrowth in mouse embryonic spinal neurons.[24] Notably, the aberrant hyperbranching of zebrafish *glra2*-depleted spinal neurons was fully rescued by human wild-type *GLRA2*, while mutant or deleted *GLRA2* failed to rescue the axon branching phenotype. This set of experiments demonstrates *in vivo* that both the deletion and R153Q mutation identified in ASD patients act through a loss-of-function mechanism, and further supports their pathogenic nature. Moreover, our approach illustrates the value of using the zebrafish as an *in vivo* tool to characterize the pathogenic impact of novel genetic variants in neurodevelopmental disorders.

The behavioral characterization of *Glra2* knockout mice showed specific impairments in short-term and long-term recognition memory in the novel object recognition task. However, their spatial learning and memory remained similar to wild-type mice when assessed in the novel location recognition task or the Morris water maze. The specific deficit in recognition memory with normal spatial learning may result from the distinct contribution of GlyR α2 in the brain regions and circuits underlying these forms of learning and memory. Although lesion and pharmacological studies indicate that the perirhinal cortex and hippocampus are necessary for object recognition memory,[44-46] analyses of neuronal activity marker expression and synaptic signaling implicate the prefrontal cortex in this form of memory.[47-49] In addition, transplantation of GABAergic precursor cells into the prefrontal cortex of mice prevents object recognition memory defects induced by the NMDA receptor antagonist phencyclidine,[50] confirming a role for the prefrontal cortex in this task and demonstrating a crucial contribution of inhibitory interneurons (see below). Thus, the memory deficit in the novel object recognition task may be the consequence of a prefrontal cortex dysfunction in *Glra2* knockout mice, a hypothesis that is supported by the altered synaptic plasticity observed in this brain region. In contrast, the absence of deficits in spatial memory suggests that the loss of *Glra2* does not affect relevant hippocampal functions. Altogether, the phenotype of *Glra2* knockout mice is in keeping with the observation that individuals with ASD typically have preserved visuospatial abilities but exhibit deficits in executive function, especially in attention and working memory.[38,51]

In humans and mice, *GLRA2* expression increases rapidly in the cortex during embryonic development, then decreases after birth and remains low in the adult (Supplementary Figure S9). This spatiotemporal pattern, along with the developmental shift from excitatory to inhibitory action of GlyRs,[14] suggests a functional role of GlyR α2 in cortical development. Interestingly, disruption of *Glra2* in mice leads to marked deficits in tangential interneuron

migration in the developing cerebral cortex.[25] This observation could provide a mechanistic substrate underlying the synaptic dysfunction and aberrant learning and memory behavior we observed in adult *Glra2* mutant mice. These results are in line with a growing body of evidence that supports a link between dysfunction of cortical inhibitory circuits and neuropsychiatric disorders, including epilepsy, schizophrenia, autism, and intellectual disability.[52] Recent studies in animal models of ASD revealed specific interneuron defects and abnormal inhibitory neurotransmission (e.g., *Nlgn3*, *Cntnap2*, *Fmr1*, and *Mecp2*).[52-55] Significantly, whereas GABAergic neurotransmission has been repeatedly implicated in models of autism,[54,56,57] the present work implicates the glycinergic system as a novel pathophysiological mechanism in ASD. GlyR α2 has also been shown to play a role in the development of excitatory projection neurons in the cortex, since *Glra2* knockout in mice impairs the proliferation and specification of cortical progenitors and leads to a reduction of cortical projection neurons[26]. These results further extend the role of *GLRA2* in different aspects of cortical development, including proliferation, differentiation, and cell migration. The disruption of *GLRA2* is likely to result in an imbalance between excitation and inhibition, by the inability to provide appropriate inhibition or excitation in cortical neuronal networks. Disruption of the excitatory-inhibitory circuit balance has emerged as a common neurophysiological substrate underlying ASD and other neurodevelopmental disorders,[58,59] a hypothesis supported by experimental observations in animal models.[52,60-62]

Hyperekplexia is a rare neurological disorder characterized by exaggerated startle responses to auditory or tactile stimuli, and neonatal hypertonia. Three major genes have been implicated: the GlyR subunits *GLRA1* and *GLRB*, and the presynaptic glycine transporter type 2, *SLC6A5*, with both dominant and recessive mutations reported.[42] Although classically considered a neuromotor disorder with normal cognitive function, recent studies in hyperekplexia have shown that learning difficulties and developmental delay are frequent, present in 40%-80% of subjects, depending on the affected gene and the mode of inheritance.[11] In particular, speech acquisition is frequently delayed. These findings strongly support the role of glycinergic transmission in neurocognitive development.

In conclusion, we used a combination of genetics and functional studies to demonstrate that *GLRA2* mutations resulting in loss of function are associated with ASD, language delay, and cognitive impairment in humans. Our *in vivo* studies of *GLRA2* in zebrafish and mice uncovered novel biological roles of this gene beyond neurotransmission, in axon branching, cognition, and synaptic plasticity. We anticipate that screening of large cohorts of individuals with ASD and other neurodevelopmental conditions will identify additional *GLRA2* mutations, as illustrated by the *de novo* missense mutation (p.N136S) in *GLRA2* found in a male with ASD in a recent whole-exome sequencing study.[5] We show here that this novel mutation substantially reduced surface expression (Supplementary Figure S4) and glycine sensitivity (Supplementary Figure S11). In agreement with these findings, mutagenesis studies identified the equivalent residue in *GLRA1*, p.N130 (p.N102 when numbered without the signal peptide) to be crucial for ligand binding.[63] Overall, our findings provide new insights into the biological roles of *GLRA2*, and implicate altered GlyR α2-dependent mechanisms in ASD-related phenotypes.

CONFLICT OF INTEREST

The authors declare no conflict of interest.

ACKNOWLEDGEMENTS

We are grateful to the families for their participation. We thank Marika Nosten-Bertrand and Stéphanie Daumas for advice on behavioral analyses, Joseph D. Buxbaum for helpful discussions, Laïla Gasmi for technical help, Guillaume Pezeron and Isabelle Anselme for help with zebrafish *in situ* hybridization experiments, Annie Munier for technical support at the Flow Cytometry Facility of the Saint-Antoine Research Center (UPMC), the Institute of Biology Paris-Seine Imaging facility, the DNA and cell bank of the Pitié-Salpêtrière Hospital, and the Clinical Investigation Center of the Robert Debré Hospital. This work was supported by a NARSAD Independent Investigator Award from the Brain & Behavior Research Foundation to CB, the Foundation for Autism Research, INSERM, CNRS and UPMC. GN and CG were supported by the Swedish Science Council and by the Annmari and Per Ahlqvist Foundation, RJH and TND by the Medical Research Council (G0500833), JCM by the Bundesministerium für Bildung und Forschung BMBF (Era-Net NEURON II CIPRESS), and MT by a Medical Research Council Centenary Award (G0600084), BBSRC (BB/K01692X/1), and the Leverhulme Trust (RPG-2012-519). MP and ED were supported by PhD fellowships from the French Ministry of Research. We gratefully acknowledge the CNV resources provided by the Autism Genome Project consortium, funded by Autism Speaks, the Health Research Board of Ireland, the Medical Research Council, Genome Canada/Ontario Genomics Institute, and the Hilibrand Foundation.

AUTHOR CONTRIBUTIONS

MP and CB conceived and designed the study; MP and AP performed sequencing experiments and variant confirmation; ED participated in the genetic analyses; BA, VG, FD, GN, MR, RD, CG and ML participated in subject recruitment and assessment; JCM provided critical reagents and advice; MP and SG performed site-directed mutagenesis; MP and HLC performed the immunohistochemistry; HLC and PL performed the *in vitro* electrophysiology studies; SDG performed the biotinylation experiments; VMJ, MT and RJH performed molecular modeling; MP, CF and JH performed the zebrafish experiments; TND and RJH generated *Glra2* knockout mice; MP performed the behavioral experiments and analyzed the results with CB; HC contributed to mouse breeding and behavioral analyses; JB and SO performed the *ex vivo* electrophysiology studies; BG provided key facilities and equipment and consulted on the execution and interpretation of the behavioral and electrophysiological studies; CB coordinated the study; MP and CB wrote the manuscript. All authors reviewed and approved the manuscript.

REFERENCES

1. Sanders SJ, Ercan-Sencicek AG, Hus V, Luo R, Murtha MT, Moreno-De-Luca D *et al.* Multiple recurrent de novo CNVs, including duplications of the 7q11.23 Williams syndrome region, are strongly associated with autism. *Neuron* 2011; **70:** 863-885.
2. Betancur C. Etiological heterogeneity in autism spectrum disorders: more than 100 genetic and genomic disorders and still counting. *Brain Res* 2011; **1380:** 42-77.
3. Pinto D, Delaby E, Merico D, Barbosa M, Merikangas A, Klei L *et al.* Convergence of genes and cellular pathways dysregulated in autism spectrum disorders. *Am J Hum Genet* 2014; **94:** 677-694.
4. De Rubeis S, He X, Goldberg AP, Poultney CS, Samocha K, Kou Y *et al.* Synaptic, transcriptional and chromatin genes disrupted in autism. *Nature* 2014; **515:** 209-215.
5. Iossifov I, O'Roak BJ, Sanders SJ, Ronemus M, Krumm N, Levy D *et al.* The contribution of de novo coding mutations to autism spectrum disorder. *Nature* 2014; **515:** 216-221.
6. Lubs HA, Stevenson RE, Schwartz CE. Fragile X and X-linked intellectual disability: four decades of discovery. *Am J Hum Genet* 2012; **90:** 579-590.
7. Ebert DH, Greenberg ME. Activity-dependent neuronal signalling and autism spectrum disorder. *Nature* 2013; **493:** 327-337.
8. Lynch JW. Native glycine receptor subtypes and their physiological roles. *Neuropharmacology* 2009; **56:** 303-309.
9. Malosio ML, Marqueze-Pouey B, Kuhse J, Betz H. Widespread expression of glycine receptor subunit mRNAs in the adult and developing rat brain. *EMBO J* 1991; **10:** 2401-2409.
10. Kang HJ, Kawasawa YI, Cheng F, Zhu Y, Xu X, Li M *et al.* Spatio-temporal transcriptome of the human brain. *Nature* 2011; **478:** 483-489.

11. Thomas RH, Chung SK, Wood SE, Cushion TD, Drew CJ, Hammond CL *et al.* Genotype-phenotype correlations in hyperekplexia: apnoeas, learning difficulties and speech delay. *Brain* 2013; **136:** 3085-3095.
12. Harvey RJ, Depner UB, Wassle H, Ahmadi S, Heindl C, Reinold H *et al.* GlyR alpha3: an essential target for spinal PGE2-mediated inflammatory pain sensitization. *Science* 2004; **304:** 884-887.
13. Winkelmann A, Maggio N, Eller J, Caliskan G, Semtner M, Haussler U *et al.* Changes in neural network homeostasis trigger neuropsychiatric symptoms. *J Clin Invest* 2014; **124:** 696-711.
14. Flint AC, Liu X, Kriegstein AR. Nonsynaptic glycine receptor activation during early neocortical development. *Neuron* 1998; **20:** 43-53.
15. Ben-Ari Y. Excitatory actions of GABA during development: the nature of the nurture. *Nat Rev Neurosci* 2002; **3:** 728-739.
16. Demarque M, Represa A, Becq H, Khalilov I, Ben-Ari Y, Aniksztejn L. Paracrine intercellular communication by a Ca^{2+}- and SNARE-independent release of GABA and glutamate prior to synapse formation. *Neuron* 2002; **36:** 1051-1061.
17. Scain AL, Le Corronc H, Allain AE, Muller E, Rigo JM, Meyrand P *et al.* Glycine release from radial cells modulates the spontaneous activity and its propagation during early spinal cord development. *J Neurosci* 2010; **30:** 390-403.
18. Spitzer NC. Electrical activity in early neuronal development. *Nature* 2006; **444:** 707-712.
19. LoTurco JJ, Owens DF, Heath MJ, Davis MB, Kriegstein AR. GABA and glutamate depolarize cortical progenitor cells and inhibit DNA synthesis. *Neuron* 1995; **15:** 1287-1298.
20. Manent JB, Demarque M, Jorquera I, Pellegrino C, Ben-Ari Y, Aniksztejn L *et al.* A noncanonical release of GABA and glutamate modulates neuronal migration. *J Neurosci* 2005; **25:** 4755-4765.
21. Bortone D, Polleux F. KCC2 expression promotes the termination of cortical interneuron migration in a voltage-sensitive calcium-dependent manner. *Neuron* 2009; **62:** 53-71.
22. Sanes DH, Chokshi P. Glycinergic transmission influences the development of dendrite shape. *Neuroreport* 1992; **3:** 323-326.
23. Furuya S, Tabata T, Mitoma J, Yamada K, Yamasaki M, Makino A *et al.* L-serine and glycine serve as major astroglia-derived trophic factors for cerebellar Purkinje neurons. *Proc Natl Acad Sci USA* 2000; **97:** 11528-11533.
24. Tapia JC, Mentis GZ, Navarrete R, Nualart F, Figueroa E, Sanchez A *et al.* Early expression of glycine and $GABA_A$ receptors in developing spinal cord neurons. Effects on neurite outgrowth. *Neuroscience* 2001; **108:** 493-506.
25. Avila A, Vidal PM, Dear TN, Harvey RJ, Rigo JM, Nguyen L. Glycine receptor α2 subunit activation promotes cortical interneuron migration. *Cell Rep* 2013; **4:** 738-750.
26. Avila A, Vidal PM, Tielens S, Morelli G, Laguesse S, Harvey RJ *et al.* Glycine receptors control the generation of projection neurons in the developing cerebral cortex. *Cell Death Differ* 2014; **21:** 1696-1708.
27. Young TL, Cepko CL. A role for ligand-gated ion channels in rod photoreceptor development. *Neuron* 2004; **41:** 867-879.
28. Pinto D, Pagnamenta AT, Klei L, Anney R, Merico D, Regan R *et al.* Functional impact of global rare copy number variation in autism spectrum disorders. *Nature* 2010; **466:** 368-372.
29. Durand CM, Betancur C, Boeckers TM, Bockmann J, Chaste P, Fauchereau F *et al.* Mutations in the gene encoding the synaptic scaffolding protein SHANK3 are associated with autism spectrum disorders. *Nat Genet* 2007; **39:** 25-27.
30. Gillberg C, Gillberg C, Rastam M, Wentz E. The Asperger Syndrome (and high-functioning autism) Diagnostic Interview (ASDI): a preliminary study of a new structured clinical interview. *Autism* 2001; **5:** 57-66.
31. Soding J, Biegert A, Lupas AN. The HHpred interactive server for protein homology detection and structure prediction. *Nucleic Acids Res* 2005; **33:** W244-248.
32. Pless SA, Hanek AP, Price KL, Lynch JW, Lester HA, Dougherty DA *et al.* A cation-pi interaction at a phenylalanine residue in the glycine receptor binding site is conserved for different agonists. *Mol Pharmacol* 2011; **79:** 742-748.
33. Bai J, Blot K, Tzavara E, Nosten-Bertrand M, Giros B, Otani S. Inhibition of dopamine transporter activity impairs synaptic depression in rat prefrontal cortex through over-stimulation of D1 receptors. *Cereb Cortex* 2014; **24:** 945-955.
34. Yuen RK, Thiruvahindrapuram B, Merico D, Walker S, Tammimies K, Hoang N *et al.* Whole-genome sequencing of quartet families with autism spectrum disorder. *Nat Med* 2015; **21:** 185-191.
35. Piton A, Gauthier J, Hamdan FF, Lafreniere RG, Yang Y, Henrion E *et al.* Systematic resequencing of X-chromosome synaptic genes in autism spectrum disorder and schizophrenia. *Mol Psychiatry* 2011; **16:** 867-880.
36. Villmann C, Oertel J, Melzer N, Becker CM. Recessive hyperekplexia mutations of the glycine receptor alpha1 subunit affect cell surface integration and stability. *J Neurochem* 2009; **111:** 837-847.
37. Koshino H, Kana RK, Keller TA, Cherkassky VL, Minshew NJ, Just MA. fMRI investigation of working memory for faces in autism: visual coding and underconnectivity with frontal areas. *Cereb Cortex* 2008; **18:** 289-300.
38. Sahyoun CP, Belliveau JW, Soulieres I, Schwartz S, Mody M. Neuroimaging of the functional and structural networks underlying visuospatial vs. linguistic reasoning in high-functioning autism. *Neuropsychologia* 2010; **48:** 86-95.
39. Stoner R, Chow ML, Boyle MP, Sunkin SM, Mouton PR, Roy S *et al.* Patches of disorganization in the neocortex of children with autism. *N Engl J Med* 2014; **370:** 1209-1219.
40. Grudzinska J, Schemm R, Haeger S, Nicke A, Schmalzing G, Betz H *et al.* The beta subunit determines the ligand binding properties of synaptic glycine receptors. *Neuron* 2005; **45:** 727-739.
41. Todorovic J, Welsh BT, Bertaccini EJ, Trudell JR, Mihic SJ. Disruption of an intersubunit electrostatic bond is a critical step in glycine receptor activation. *Proc Natl Acad Sci USA* 2010; **107:** 7987-7992.

42. Bode A, Lynch JW. The impact of human hyperekplexia mutations on glycine receptor structure and function. *Mol Brain* 2014; **7:** 2.
43. Kabashi E, Champagne N, Brustein E, Drapeau P. In the swim of things: recent insights to neurogenetic disorders from zebrafish. *Trends Genet* 2010; **26:** 373-381.
44. Warburton EC, Brown MW. Findings from animals concerning when interactions between perirhinal cortex, hippocampus and medial prefrontal cortex are necessary for recognition memory. *Neuropsychologia* 2010; **48:** 2262-2272.
45. Brown MW, Barker GR, Aggleton JP, Warburton EC. What pharmacological interventions indicate concerning the role of the perirhinal cortex in recognition memory. *Neuropsychologia* 2012; **50:** 3122-3140.
46. Cohen SJ, Munchow AH, Rios LM, Zhang G, Asgeirsdottir HN, Stackman RW, Jr. The rodent hippocampus is essential for nonspatial object memory. *Curr Biol* 2013; **23:** 1685-1690.
47. Nagai T, Takuma K, Kamei H, Ito Y, Nakamichi N, Ibi D *et al.* Dopamine D1 receptors regulate protein synthesis-dependent long-term recognition memory via extracellular signal-regulated kinase 1/2 in the prefrontal cortex. *Learn Mem* 2007; **14:** 117-125.
48. Rinaldi A, Romeo S, Agustin-Pavon C, Oliverio A, Mele A. Distinct patterns of Fos immunoreactivity in striatum and hippocampus induced by different kinds of novelty in mice. *Neurobiol Learn Mem* 2010; **94:** 373-381.
49. Barbosa FF, Santos JR, Meurer YS, Macedo PT, Ferreira LM, Pontes IM *et al.* Differential cortical c-Fos and Zif-268 expression after object and spatial memory processing in a standard or episodic-like object recognition task. *Front Behav Neurosci* 2013; **7:** 112.
50. Tanaka DH, Toriumi K, Kubo K, Nabeshima T, Nakajima K. GABAergic precursor transplantation into the prefrontal cortex prevents phencyclidine-induced cognitive deficits. *J Neurosci* 2011; **31:** 14116-14125.
51. Fan J. Attentional network deficits in autism spectrum disorders. In: Buxbaum JD, Hof PR (eds). *The Emerging Neuroscience of Autism Spectrum Disorders*. Elsevier: Oxford, UK, 2011, pp 281-288.
52. Marin O. Interneuron dysfunction in psychiatric disorders. *Nat Rev Neurosci* 2012; **13:** 107-120.
53. Tabuchi K, Blundell J, Etherton MR, Hammer RE, Liu X, Powell CM *et al.* A neuroligin-3 mutation implicated in autism increases inhibitory synaptic transmission in mice. *Science* 2007; **318:** 71-76.
54. Chao HT, Chen H, Samaco RC, Xue M, Chahrour M, Yoo J *et al.* Dysfunction in GABA signalling mediates autism-like stereotypies and Rett syndrome phenotypes. *Nature* 2010; **468:** 263-269.
55. Penagarikano O, Abrahams BS, Herman EI, Winden KD, Gdalyahu A, Dong H *et al.* Absence of CNTNAP2 leads to epilepsy, neuronal migration abnormalities, and core autism-related deficits. *Cell* 2011; **147:** 235-246.
56. Paluszkiewicz SM, Martin BS, Huntsman MM. Fragile X syndrome: the GABAergic system and circuit dysfunction. *Dev Neurosci* 2011; **33:** 349-364.
57. Han S, Tai C, Westenbroek RE, Yu FH, Cheah CS, Potter GB *et al.* Autistic-like behaviour in *Scn1a*$^{+/-}$ mice and rescue by enhanced GABA-mediated neurotransmission. *Nature* 2012; **489:** 385-390.
58. Rubenstein JL, Merzenich MM. Model of autism: increased ratio of excitation/inhibition in key neural systems. *Genes Brain Behav* 2003; **2:** 255-267.
59. Rubenstein JL. Three hypotheses for developmental defects that may underlie some forms of autism spectrum disorder. *Curr Opin Neurol* 2010; **23:** 118-123.
60. Gogolla N, Leblanc JJ, Quast KB, Sudhof TC, Fagiolini M, Hensch TK. Common circuit defect of excitatory-inhibitory balance in mouse models of autism. *J Neurodev Disord* 2009; **1:** 172-181.
61. Yizhar O, Fenno LE, Prigge M, Schneider F, Davidson TJ, O'Shea DJ *et al.* Neocortical excitation/inhibition balance in information processing and social dysfunction. *Nature* 2011; **477:** 171-178.
62. Sudhof TC. Neuroligins and neurexins link synaptic function to cognitive disease. *Nature* 2008; **455:** 903-911.
63. Vafa B, Lewis TM, Cunningham AM, Jacques P, Lynch JW, Schofield PR. Identification of a new ligand binding domain in the alpha1 subunit of the inhibitory glycine receptor. *J Neurochem* 1999; **73:** 2158-2166.

Supplementary Information accompanies the paper on the Molecular Psychiatry website (http://www.nature.com/mp)

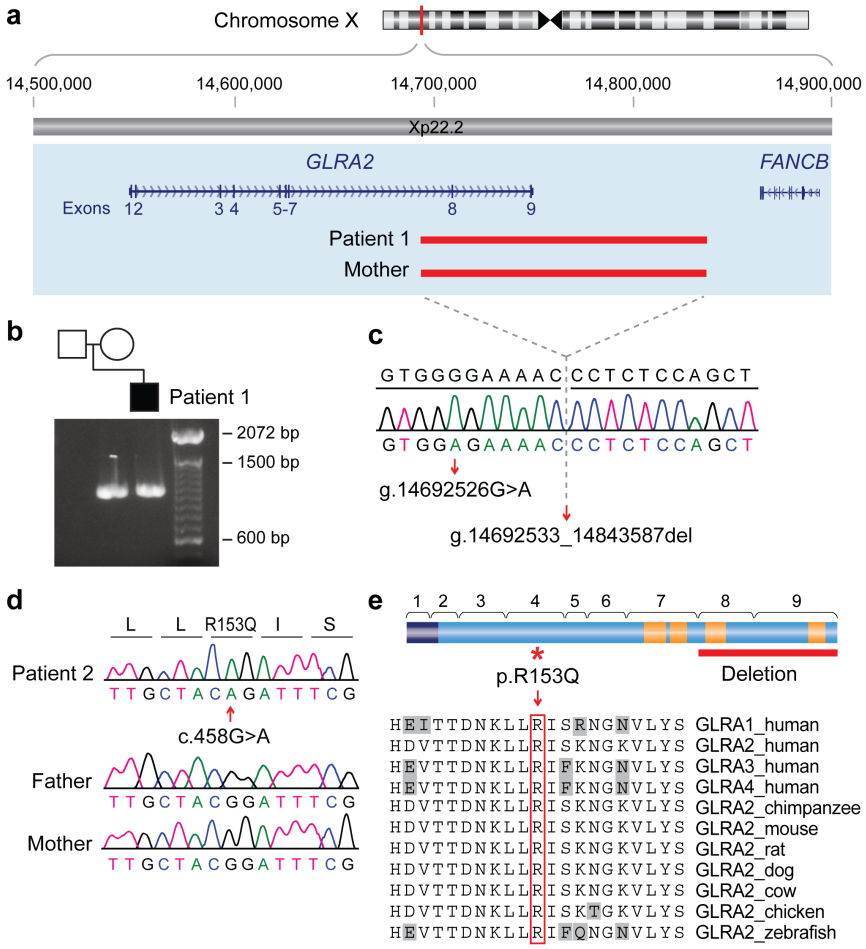

Figure 1. Microdeletion and mutation of *GLRA2* in ASD. (**a**) Physical map of Xp22.2. CNV analysis showed a *GLRA2* deletion removing exons 8 and 9 in Patient 1, inherited from his unaffected mother (red). (**b**) Gel image of long-range PCR products showing an abnormal 1.1 kb allele in Patient 1 and his mother. (**c**) Breakpoint sequence analysis in Patient 1 revealed a 151055 bp deletion starting in intron 7 of *GLRA2*. A G>A transition precedes the deletion. (**d**) Identification of a *de novo* missense mutation in exon 4 of *GLRA2* in Patient 2 (c.458G>A, p.153R>Q). (**e**) Schematic representation of the GLRA2 protein with the deletion and the mutation identified in ASD. The exons are indicated by brackets; the signal peptide and the four transmembrane domains are shown in dark blue and orange, respectively. The alignment of protein sequences of human GlyRs and orthologs from other species is shown below. The highly conserved arginine at position 153, mutated in Patient 2, is boxed in red.

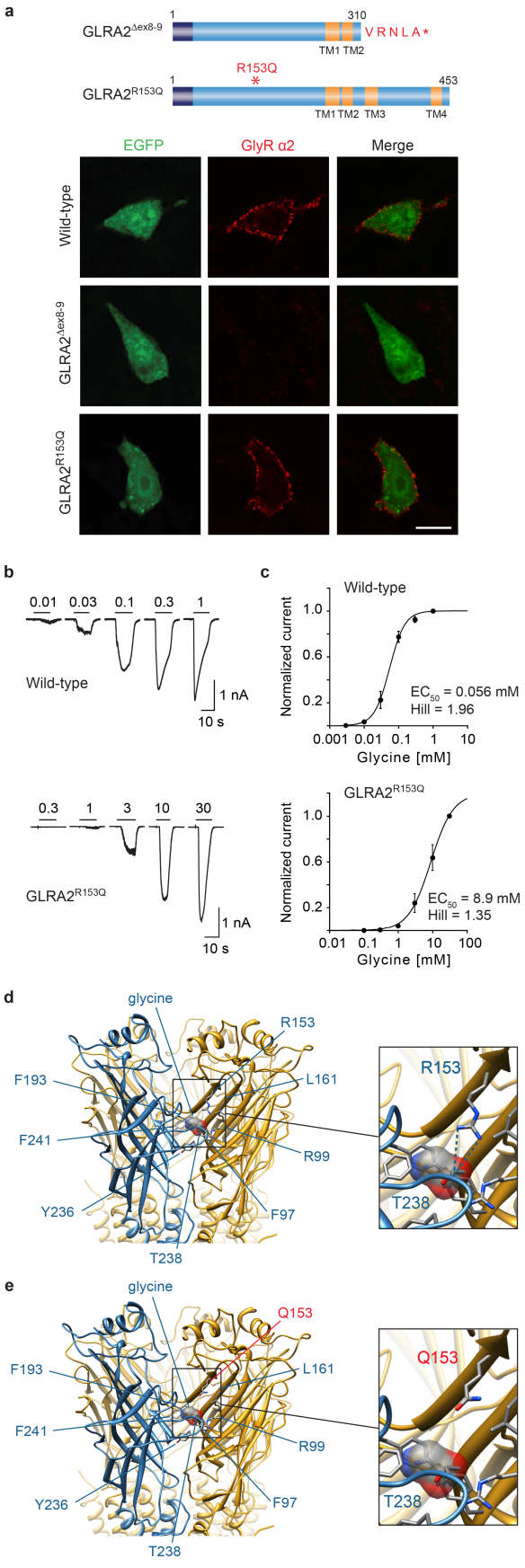

Figure 2. *GLRA2* mutations identified in individuals with ASD abolish normal protein function. (**a**) Schematic representation of deleted and mutated GLRA2 constructs co-transfected with EGFP cDNA in CHO cells. The truncated mutant (GLRA2$^{\Delta ex8\text{-}9}$) was produced to end at amino acid 310, immediately followed by six amino acids (VRNLA*), resulting in loss of two transmembrane domains, as in Patient 1. In the mutant construct (GLRA2^{R153Q}), Arg153 was mutated to glutamine as in Patient 2. The first and last amino acids are numbered; the signal peptide and the four transmembrane domains are shown in dark blue and orange, respectively. Confocal cross-sections show surface expression of wild-type and mutant GLRA2 proteins in non-permeabilized cells. GLRA2^{R153Q} localized properly to the plasma membrane, as shown by the punctiform staining of GlyR α2 at the cell surface, whereas GLRA2$^{\Delta ex8\text{-}9}$ failed to traffic to the membrane. Scale bar, 10 µm. (**b**) Representative traces of currents evoked by application of glycine on CHO cells expressing wild-type and mutated GLRA2 proteins. Bars represent application of glycine at concentrations noted. (**c**) Fit of data in (**b**) to the Hill equation. Errors indicate SEM (*n* = 7 GLRA2^{R153Q}, 13 wild-type). (**d**, **e**) Predicted structure of the homomeric GlyR α2 subunit. The blue and yellow α2 subunits contain residues on the plus and minus sides of the glycine-binding site, respectively. A single glycine-binding site is represented in the native state (**d**) and the R153Q mutant (**e**). Predicted residues of importance are labeled by residue number. Dashed lines indicate hydrogen bonds. Elimination of the hydrogen bonds stabilizing the backbone of the binding-site residue T238 is predicted to cause direct disruption of glycine binding.

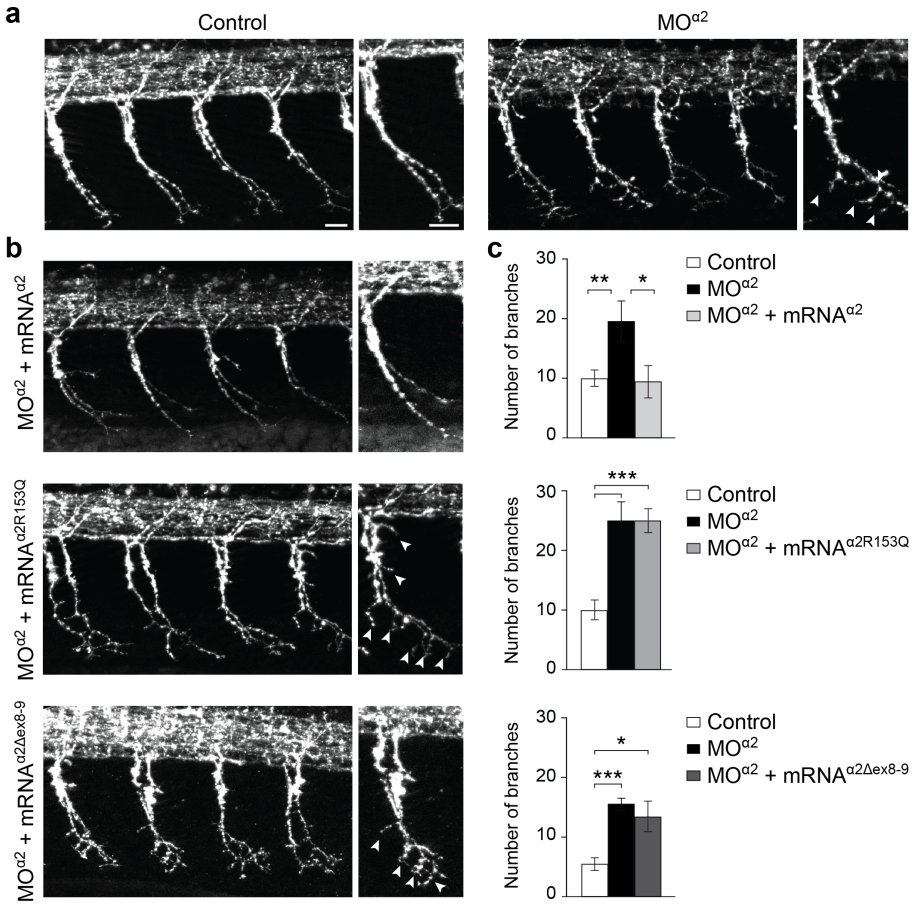

Figure 3. ASD-associated mutations in *GLRA2* fail to rescue the axon branching phenotype caused by knockdown of the zebrafish orthologue. (**a, b**) Immunostaining of 28-h post-fertilization control (**a**), morphant (MO$^{\alpha2}$) (**a**), and rescued (MO$^{\alpha2}$ + mRNA$^{\alpha2}$ or mRNA$^{\alpha2R153Q}$ or mRNA$^{\alpha2\Delta ex8-9)}$ (**b**) larvae labeled with Znp1 antibody; lateral views of the trunk (anterior to the left). Higher magnifications are shown on the right. Arrows indicate aberrant supernumerary branches of spinal motor axons. Scale bars for all images, 10 µm. (**c**) Quantification of axon branching in 16 somites centered around the anus in control, morphant, and rescued larvae. The number of branches was significantly higher in MO$^{\alpha2}$ larvae than in controls and was rescued by concomitant overexpression of human *GLRA2* (mRNA$^{\alpha2}$), whereas deleted (mRNA$^{\alpha2\Delta ex8-9}$) or mutated (mRNA$^{\alpha2R153Q}$) versions of the transcript failed to rescue the abnormal axon phenotype. Data represent mean ± SEM. **P*<0.05, ***P*<0.01, ****P*<0.001.

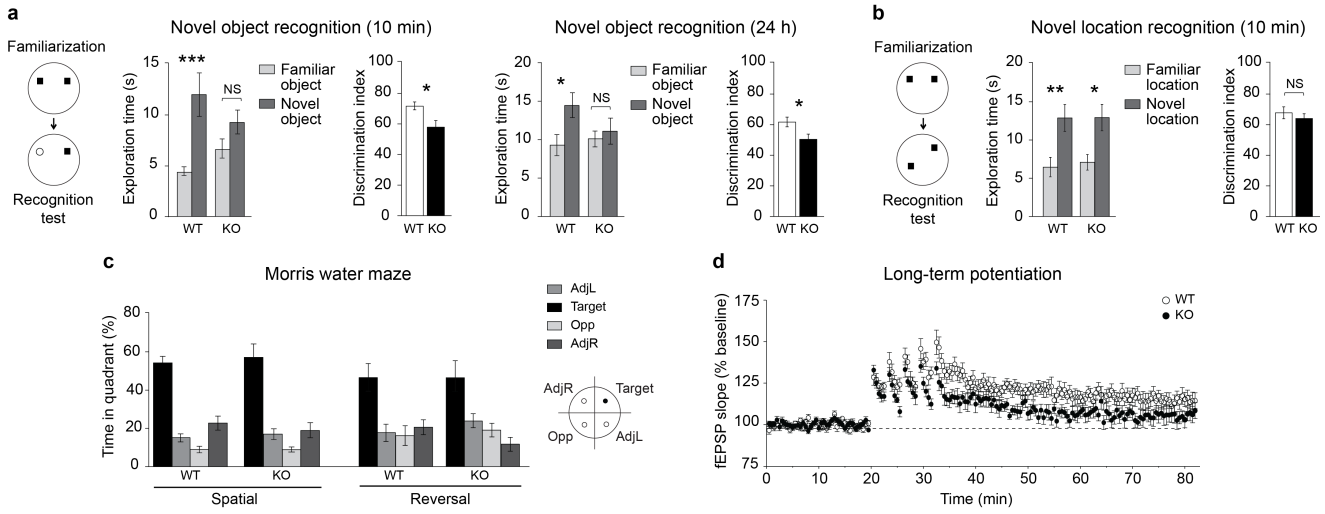

Figure 4. *Glra2*$^{-/Y}$ mice exhibit deficits in recognition memory and impaired cortical synaptic plasticity. (**a**) In the novel object recognition task, adult wild-type (WT) mice spent more time exploring the novel object, whereas *Glra2*$^{-/Y}$ mice had no preference for either object after a 10 min or 24 h memory delay, as measured by exploration time and discrimination index (n = 11 WT, 12 *Glra2*$^{-/Y}$). (**b**) *Glra2*$^{-/Y}$ mice exhibited no deficits when assessed on the spatial version of the task (the novel location recognition test) and showed normal preference for the object placed in a new location (n = 9 WT, 10 *Glra2*$^{-/Y}$). (**c**) In the Morris water maze, *Glra2*$^{-/Y}$ mice displayed normal acquisition and reversal learning. Both genotypes showed a significant preference for the target quadrant during a probe trial conducted 10 min following the final training session (n = 5 WT, 7 *Glra2*$^{-/Y}$). AdjL, adjacent left quadrant; Target, target quadrant; AdjR, adjacent right quadrant; Opp, opposite to target quadrant. (**d**) *Glra2*$^{-/Y}$ mice exhibited impaired long-term potentiation in the prefrontal cortex (n = 14 slices from 9 WT mice, 10 slices from 6 *Glra2*$^{-/Y}$ mice). fEPSP, field excitatory postsynaptic potential. Data represent mean ± SEM. *P<0.05, **P<0.01, ***P<0.001.